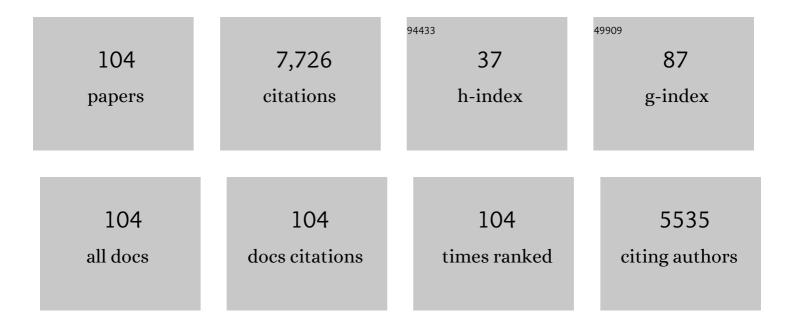
zhi-ling Hou

List of Publications by Year in descending order

Source: https://exaly.com/author-pdf/1653239/publications.pdf Version: 2024-02-01



#	Article	IF	CITATIONS
1	The effects of temperature and frequency on the dielectric properties, electromagnetic interference shielding and microwave-absorption of short carbon fiber/silica composites. Carbon, 2010, 48, 788-796.	10.3	1,582
2	Temperature dependent microwave attenuation behavior for carbon-nanotube/silica composites. Carbon, 2013, 65, 124-139.	10.3	1,009
3	Ferroferric Oxide/Multiwalled Carbon Nanotube vs Polyaniline/Ferroferric Oxide/Multiwalled Carbon Nanotube Multiheterostructures for Highly Effective Microwave Absorption. ACS Applied Materials & Interfaces, 2012, 4, 6949-6956.	8.0	823
4	Multi-wall carbon nanotubes decorated with ZnO nanocrystals: mild solution-process synthesis and highly efficient microwave absorption properties at elevated temperature. Journal of Materials Chemistry A, 2014, 2, 10540.	10.3	420
5	High dielectric loss and its monotonic dependence of conducting-dominated multiwalled carbon nanotubes/silica nanocomposite on temperature ranging from 373 to 873 K in X-band. Applied Physics Letters, 2009, 94, .	3.3	333
6	High-temperature microwave absorption and evolutionary behavior of multiwalled carbon nanotube nanocomposite. Scripta Materialia, 2009, 61, 201-204.	5.2	204
7	Multifunctional broadband microwave absorption of flexible graphene composites. Carbon, 2019, 141, 608-617.	10.3	197
8	Facile fabrication of ultrathin graphene papers for effective electromagnetic shielding. Journal of Materials Chemistry C, 2014, 2, 5057-5064.	5.5	159
9	Unusual continuous dual absorption peaks in Ca-doped BiFeO ₃ nanostructures for broadened microwave absorption. Nanoscale, 2016, 8, 10415-10424.	5.6	147
10	Silicon carbide powders: Temperature-dependent dielectric properties and enhanced microwave absorption at gigahertz range. Solid State Communications, 2013, 163, 1-6.	1.9	133
11	Synthesis of zinc oxide particles coated multiwalled carbon nanotubes: Dielectric properties, electromagnetic interference shielding and microwave absorption. Materials Research Bulletin, 2012, 47, 1747-1754.	5.2	122
12	Boron Nitride Nanomaterials for Thermal Management Applications. ChemPhysChem, 2015, 16, 1339-1346.	2.1	119
13	Construction of caterpillar-like hierarchically structured Co/MnO/CNTs derived from MnO2/ZIF-8@ZIF-67 for electromagnetic wave absorption. Carbon, 2021, 173, 521-527.	10.3	114
14	A wearable microwave absorption cloth. Journal of Materials Chemistry C, 2017, 5, 2432-2441.	5.5	100
15	Flexible Graphene–Graphene Composites of Superior Thermal and Electrical Transport Properties. ACS Applied Materials & Interfaces, 2014, 6, 15026-15032.	8.0	97
16	Ultrathin Topological Insulator Absorber: Unique Dielectric Behavior of Bi ₂ Te ₃ Nanosheets Based on Conducting Surface States. ACS Applied Materials & Interfaces, 2019, 11, 33285-33291.	8.0	94
17	Alignment of graphene sheets in wax composites for electromagnetic interference shielding improvement. Nanotechnology, 2013, 24, 115708.	2.6	87
18	Multi-dimensional flexible reduced graphene oxide/polymer sponges for multiple forms of strain sensors. Carbon, 2017, 125, 199-206.	10.3	83

#	Article	IF	CITATIONS
19	Enhanced ferromagnetism and microwave absorption properties of BiFeO3 nanocrystals with Ho substitution. Materials Letters, 2012, 84, 110-113.	2.6	82
20	Ni-decorated SiC powders: Enhanced high-temperature dielectric properties and microwave absorption performance. Powder Technology, 2013, 237, 309-313.	4.2	75
21	Enhanced fluorescence properties of carbon dots in polymer films. Journal of Materials Chemistry C, 2016, 4, 6967-6974.	5.5	74
22	Lightweight ferroferric oxide nanotubes with natural resonance property and design for broadband microwave absorption. Journal of Materials Science, 2017, 52, 8258-8267.	3.7	64
23	Layer by layer 2D MoS2/rGO hybrids: An optimized microwave absorber for high-efficient microwave absorption. Applied Surface Science, 2019, 470, 899-907.	6.1	62
24	A universal permittivity-attenuation evaluation diagram for accelerating design of dielectric-based microwave absorption materials: A case of graphene-based composites. Carbon, 2017, 118, 86-97.	10.3	61
25	Microwave permittivity and permeability experiments in high-loss dielectrics: Caution with implicit Fabry-Pérot resonance for negative imaginary permeability. Applied Physics Letters, 2013, 103, .	3.3	58
26	Biopolymer nanofiber/reduced graphene oxide aerogels for tunable and broadband high-performance microwave absorption. Composites Part B: Engineering, 2019, 161, 1-9.	12.0	57
27	Microwave responses and general model of nanotetraneedle ZnO: Integration of interface scattering, microcurrent, dielectric relaxation, and microantenna. Journal of Applied Physics, 2010, 107, 054304.	2.5	53
28	High-temperature conductance loss dominated defect level in h-BN: Experiments and first principles calculations. Journal of Applied Physics, 2009, 105, .	2.5	50
29	High dielectric loss and microwave absorption behavior of multiferroic BiFeO 3 ceramic. Ceramics International, 2013, 39, 7241-7246.	4.8	49
30	Flexible Semitransparent Energy Harvester with High Pressure Sensitivity and Power Density Based on Laterally Aligned PZT Single-Crystal Nanowires. ACS Applied Materials & Interfaces, 2017, 9, 24696-24703.	8.0	48
31	Structure, ferromagnetism and microwave absorption properties of La substituted BiFeO3 nanoparticles. Materials Letters, 2013, 111, 130-133.	2.6	47
32	Structural stability, electronic and optical properties of Ni-doped 3C–SiC by first principles calculation. Journal of Alloys and Compounds, 2011, 509, 6117-6122.	5.5	46
33	Electrospinning fabrication and ultra-wideband electromagnetic wave absorption properties of CeO2/N-doped carbon nanofibers. Nano Research, 2022, 15, 7788-7796.	10.4	44
34	Enhanced magnetization and improved leakage in Erâ€doped BiFeO ₃ nanoparticles. Physica Status Solidi (A) Applications and Materials Science, 2013, 210, 809-813.	1.8	43
35	Mutual promotion effect of Pr and Mg co-substitution on structure and multiferroic properties of BiFeO3 ceramic. Ceramics International, 2017, 43, 262-267.	4.8	42
36	Fast-moving piezoelectric micro-robotic fish with double caudal fins. Robotics and Autonomous Systems, 2021, 140, 103733.	5.1	42

#	Article	IF	CITATIONS
37	Mg-substitution for promoting magnetic and ferroelectric properties of BiFeO3 multiferroic nanoparticles. Materials Letters, 2016, 175, 207-211.	2.6	40
38	Low dielectric loss and non-Debye relaxation of gamma-Y2Si2O7 ceramic at elevated temperature in X-band. Journal of Applied Physics, 2009, 105, .	2.5	38
39	A general model of dielectric constant for porous materials. Applied Physics Letters, 2016, 108, .	3.3	37
40	High sensitivity self-recovery ethanol sensor based on polyporous graphene oxide/melamine composites. Carbon, 2018, 137, 467-474.	10.3	36
41	Designing high-performance electromagnetic wave absorption materials based on polymeric graphene-based dielectric composites: from fabrication technology to periodic pattern design. Journal of Materials Chemistry C, 2017, 5, 6745-6754.	5.5	34
42	Construction of three-dimensional graphene interfaces into carbon fiber textiles for increasing deposition of nickel nanoparticles: flexible hierarchical magnetic textile composites for strong electromagnetic shielding. Nanotechnology, 2017, 28, 045710.	2.6	34
43	MXene films: Toward high-performance electromagnetic interference shielding and supercapacitor electrode. Composites Part A: Applied Science and Manufacturing, 2022, 157, 106935.	7.6	32
44	Uniform SiOx/graphene composite materials for lithium ion battery anodes. Journal of Alloys and Compounds, 2019, 809, 151798.	5.5	29
45	Beta-manganese dioxide nanorods for sufficient high-temperature electromagnetic interference shielding in X-band. Applied Physics A: Materials Science and Processing, 2014, 116, 1779-1783.	2.3	28
46	Highly sensitive humidity sensor based on graphene oxide foam. Applied Physics Letters, 2017, 111, .	3.3	28
47	High-Sensitivity and Ultrafast-Response Ethanol Sensors Based on Graphene Oxide. ACS Applied Materials & Interfaces, 2020, 12, 38708-38713.	8.0	25
48	Size-modulated electromagnetic properties and highly efficient microwave absorption of magnetic iron oxide ceramic opened-hollow microspheres. Ceramics International, 2019, 45, 23043-23049.	4.8	24
49	Nano-scale and micron-scale manganese dioxide vs corresponding paraffin composites for electromagnetic interference shielding and microwave absorption. Materials Research Bulletin, 2014, 51, 277-286.	5.2	22
50	Exceptional electrical and thermal transport properties in tunable all-graphene papers. RSC Advances, 2015, 5, 75239-75247.	3.6	22
51	Enhanced magnetization and bias voltage-dependent dielectric properties of Sm-doped BiFeO3 multiferroic nanofibers. Journal of Materials Science, 2018, 53, 10249-10260.	3.7	22
52	Scattering mechanisms and anomalous conductivity of heavily N-doped 3C-SiC in ultraviolet region. Physics Letters, Section A: General, Atomic and Solid State Physics, 2010, 374, 2286-2289.	2.1	21
53	Origin of Negative Imaginary Part of Effective Permittivity of Passive Materials. Chinese Physics Letters, 2017, 34, 097701.	3.3	21
54	Enhanced Ferromagnetism and Microwave Dielectric Properties of Bi _{0.95} Y _{0.05} FeO ₃ Nanocrystals. Chinese Physics Letters, 2011, 28, 037702.	3.3	20

#	Article	IF	CITATIONS
55	Tetra-needle zinc oxide/silica composites: High-temperature dielectric properties at X-band. Solid State Communications, 2013, 154, 64-68.	1.9	20
56	One-Step Synthesis of SiO _{<i>x</i>} @Graphene Composite Material by a Hydrothermal Method for Lithium-Ion Battery Anodes. Energy & Fuels, 2020, 34, 3895-3900.	5.1	20
57	The Comprehensive Retrieval Method of Electromagnetic Parameters Using the Scattering Parameters of Metamaterials for Two Choices of Time-Dependent Factors. Chinese Physics Letters, 2012, 29, 017701.	3.3	16
58	Graphene oxide foams: the simplest carbon-air prototypes for unique variable dielectrics. Journal of Materials Chemistry C, 2017, 5, 3397-3407.	5.5	16
59	Broadening Electromagnetic Absorption Bandwidth: Design from Microscopic Dielectricâ€Magnetic Coupled Absorbers to Macroscopic Patterns. Physica Status Solidi (A) Applications and Materials Science, 2017, 214, 1700589.	1.8	16
60	Smart mechano-hydro-dielectric coupled hybrid sponges for multifunctional sensors. Sensors and Actuators B: Chemical, 2018, 270, 239-246.	7.8	16
61	The self-consistent nonlinear theory of electron cyclotron maser based on anomalous Doppler effect. Applied Physics Letters, 2011, 98, 261502.	3.3	15
62	First Principle Study of the Electronic Properties of 3C-SiC Doped with Different Amounts of Ni. Chinese Physics Letters, 2012, 29, 077701.	3.3	15
63	Modeling for multi-resonant behavior of broadband metamaterial absorber with geometrical substrate. Chinese Physics B, 2017, 26, 127802.	1.4	15
64	Plasmonic nanosensor based on sharp Fano resonances induced by aperture-coupled slot system. Optics Communications, 2021, 480, 126438.	2.1	14
65	A highly conductive self-assembled multilayer graphene nanosheet film for electronic tattoos in the applications of human electrophysiology and strain sensing. Nanoscale, 2021, 13, 10798-10806.	5.6	14
66	Structural and thermoelectric properties of Zr-doped TiPdSn half-Heusler compound by first-principles calculations. Chemical Physics Letters, 2020, 741, 137055.	2.6	13
67	Ultrafastâ€Response Humidity Sensor with High Humidity Durability Based on a Freestanding Film of Graphene Oxide Supramolecular. Physica Status Solidi (A) Applications and Materials Science, 2020, 217, 1900869.	1.8	12
68	Highly dispersive GO-based supramolecular absorber: Chemical-reduction optimization for impedance matching. Journal of Alloys and Compounds, 2020, 834, 155122.	5.5	12
69	Sb2Te3 nanosheets: Topological insulators with extraordinary electromagnetic response behaviors. Chemical Engineering Journal, 2021, 414, 128036.	12.7	12
70	High-temperature dielectric properties and microwave absorption abilities of Bi1â^'xMgxFeO3 nanoparticles. Ceramics International, 2017, 43, 11815-11819.	4.8	11
71	Polarization Mechanism of Oxygen Vacancy and Its Influence on Dielectric Properties in ZnO. Chinese Physics Letters, 2011, 28, 027101.	3.3	10
72	Enhanced photovoltaic property based on reduced leakage current and band gap in Nd-doped BiFeO ₃ films. Materials Research Express, 2019, 6, 086426.	1.6	9

#	Article	IF	CITATIONS
73	Delicate construction of Si@SiOx composite materials by microwave hydrothermal for lithium-ion battery anodes. Ionics, 2020, 26, 69-74.	2.4	9
74	Sm doped BiFeO3 nanofibers for improved photovoltaic devices. Chinese Journal of Physics, 2020, 66, 301-306.	3.9	9
75	Rutile TiO2 nanorod with anomalous resonance for charge storage and frequency selective absorption. Ceramics International, 2021, 47, 2016-2021.	4.8	9
76	Si@Cu composite anode material prepared by magnetron sputtering for high-capacity lithium-ion batteries. International Journal of Hydrogen Energy, 2022, 47, 4766-4771.	7.1	8
77	Highly efficient and giant negative electrocaloric effect of a Nb and Sn co-doped lead zirconate titanate antiferroelectric film near room temperature. RSC Advances, 2019, 9, 34114-34119.	3.6	7
78	Metal-organic frameworks derived carbon nanotube and carbonyl iron composite materials for broadband microwave absorbers with a wide filling range. Journal of Magnetism and Magnetic Materials, 2022, 555, 169391.	2.3	7
79	Electronic scattering leads to anomalous thermal conductivity of n-type cubic silicon carbide in the high-temperature region. Journal of Physics Condensed Matter, 2012, 24, 445802.	1.8	6
80	High-Temperature Permittivity and Data-Mining of Silicon Dioxide at GHz Band. Chinese Physics Letters, 2012, 29, 027701.	3.3	6
81	Nanoscale polygonal carbon: a unique low-loading filler for effective microwave absorption. Journal of Materials Science: Materials in Electronics, 2016, 27, 8159-8168.	2.2	6
82	Wide-domain controlled electromagnetic and microwave absorption properties of PANI/Ni _{0.5} Zn _{0.5} Fe ₂ O ₄ composites. Materials Research Express, 2017, 4, 075029.	1.6	6
83	Low-loss near-zero-index metamaterial based on a single board for broadband electromagnetic-wave switches. Optics Communications, 2019, 446, 113-117.	2.1	6
84	A highly directional metamaterial-based terahertz circulator that does not require an external magnetic field. Journal Physics D: Applied Physics, 2021, 54, 105103.	2.8	6
85	Graphene and Carbon Nanotube Dual-Decorated SiO _{<i>x</i>} Composite Anode Material for Lithium-Ion Batteries. Energy & Fuels, 2021, 35, 19784-19790.	5.1	6
86	The novel structure and superconductivity of zirconium hydride. Computational Materials Science, 2017, 134, 38-41.	3.0	5
87	Loaded Slot Cavity Induced Sensing Enhancement and Transparency Based on Plasmonic Structure. IEEE Sensors Journal, 2022, 22, 14044-14050.	4.7	5
88	A low-reflection coaxial tunable attenuator based on zero refractive index metamaterial. Journal of Applied Physics, 2016, 120, 183102.	2.5	4
89	Plasmon-Induced Transparency for Tunable Atom Trapping in a Chiral Metamaterial Structure. Nanomaterials, 2022, 12, 516.	4.1	4
90	Different Roles of a Boron Substitute for Carbon and Silicon in β-SiC. Chinese Physics Letters, 2012, 29, 077102.	3.3	3

#	Article	IF	CITATIONS
91	The resonance interaction of relativistic charged particle and circularly polarized electromagnetic wave. Communications in Nonlinear Science and Numerical Simulation, 2012, 17, 1104-1106.	3.3	3
92	The nonlinear theory of slow-wave electron cyclotron masers with inclusion of the beam velocity spread. Annals of Physics, 2013, 339, 588-595.	2.8	3
93	Efficiency enhancement of anomalous-Doppler electron cyclotron masers with tapered magnetic field. Physics of Plasmas, 2014, 21, 023117.	1.9	3
94	Preparation of Fe ₃ O ₄ nanospindle composites and high performance microwave absorption. Chinese Science Bulletin, 2018, 63, 3667-3676.	0.7	3
95	Microwave Absorption and Mechanical Properties of CNTs/ PU Composites with Honeycomb Structure. Applied Composite Materials, 2022, 29, 1393-1407.	2.5	3
96	Enhancing the efficiency of slow-wave electron cyclotron masers with the tapered refractive index. Physics of Plasmas, 2013, 20, 043107.	1.9	2
97	Towards nanostructured boron nitride films. Journal of Materials Science: Materials in Electronics, 2017, 28, 9048-9055.	2.2	2
98	Preparation and absorption performance of CNTs/PUR honeycomb composite absorbing material. Journal of Physics: Conference Series, 2021, 2076, 012026.	0.4	2
99	Numerical Simulations of Nonlinear Dynamics of Electron Cyclotron Maser with a Straight Beam. Chinese Physics Letters, 2011, 28, 117702.	3.3	1
100	A density-functional theory investigation on desorption of O 2 on Sn(111) and its comparison with initial oxidation on the X (111) (X = Si, Ge, Sn, Pb) surfaces. Chinese Physics B, 2012, 21, 126803.	1.4	1
101	The Self-Consistent Nonlinear Theory of Charged Particle Beam Acceleration by Slowed Circularly Polarized Electromagnetic Waves. Plasma Science and Technology, 2013, 15, 1174-1177.	1.5	1
102	Ultra-unidirectional Emission with Enhanced Spectral Splitting Based on Plasmonic Nano-pillars and its Metasurface. Plasmonics, 2022, 17, 1463-1469.	3.4	1
103	Highly tunable directional optical antennas with large local angular chiroptical effects. Journal of Applied Physics, 2022, 131, 033103.	2.5	0
104	Distinct local angular chiroptical effects with unidirectional emission based on asymmetric plasmonic nanopillar antennas. Optics Communications, 2022, 514, 128122.	2.1	0